Journal of Statistical Physics, Vol. 66, Nos. 3/4, 1992

Phase Separation Dynamics in Driven Diffusive Systems

C. Yeung,[1] T. Rogers,[1] A. Hernandez-Machado,[1,2] and David Jasnow[1]

Received August 20, 1991

We study phase separation dynamics in a driven diffusive system. Our simulations are based on the Cahn–Hilliard equation with an additional flux term due to an external field. We study the dynamical scaling parallel and perpendicular to the field. A crossover is observed from isotropic domains at early times to extremely anisotropic domains at later times. We find that the inverse interfacial density (an isotropic measure of the domain size) increases as t^{α}, with $\alpha = 1/3$, from early times independent of the field strength, even though we do not observe dynamical scaling during these times. Our results indicate that a growth exponent $\alpha = 1/3$ may be more universal than previously expected. We analyze the dynamics in terms of surface driven instabilities and one-dimensional solitary waves.

KEY WORDS: Nonequilibrium steady state; driven diffusive systems; phase ordering dynamics; interfacial instabilities.

1. INTRODUCTION

Driven diffusive systems are useful paradigms in understanding many aspects of nonequilibrium physics.[1] Examples include fast ionic conductors[2] and phase transitions in the presence of a gravitational, magnetic, or electric field. The simplest model of a driven diffusive system is a lattice gas in the presence of an external field which enchances the transition rates along the field direction. For periodic boundary conditions, the system evolves to a constant-current steady state.[3] For attractive interparticle interactions, there is a sharp transition with decreasing temperature from a

[1] Department of Physics and Astronomy, University of Pittsburgh, Pittsburgh, Pennsylvania 15260.

[2] Permanent address: Departamento ECM, Facultad de Física, Universitat de Barcelona, E-08028 Barcelona, Spain.

822/66/3-4-25

single-phase regime to one of two-phase coexistence. In the latter regime, low- and high-density domains are separated by an interface whose orientation is determined by the direction of the field and the boundary conditions. This nonequilibrium phase transition has been studied both by computer simulations[3,4] and analytical methods.[5–8] More recently, driven diffusive systems have also become useful tools in the study of nonequilibrium dynamics of interfaces, such as the generation and growth of structures in the presence of an external field.[9,10] Various types of instabilities have been proposed to understand the morphologies obtained in different cases.[11–14] These studies have been helpful in developing an understanding of the dynamics of systems far from equilibrium.

There has also been interest in the means by which a system approaches two-phase equilibrium after a rapid quench from the single-phase regime (see refs. 15 for reviews). For zero field, the phase separation dynamics displays dynamical scaling and a large degree of universality. The scaling behavior, which depends on the universality class of the dynamics, can be specified by a few dynamical exponents and by the scaling form of the scattering intensity. The case relevant to this paper is phase separation dynamics for a conserved order parameter without hydrodynamics. In this case, for zero field, the characteristic domain size grows as $t^{1/3}$, where t is the time after the quench. However, it is not known how the field affects the universality class of the phase separation process.

In this paper we combine these ideas and methodologies to study the behavior of driven diffusive systems (DDS) after a rapid quench into the two-phase regime. We perform two-dimensional numerical simulations to investigate the effect of a field-induced anisotropy on growth and dynamical scaling. Our studies are motivated from a practical point of view. For example, a gravitational field is present in most experiments, and although this effect is important at late times, there has been little theoretical analysis.[16] Furthermore, for the single-phase regime, it has been shown that anisotropy is a singular perturbation, changing the character of the correlation function from exponential decay to power-law decay at long distances.[17] It is, therefore, important both for experimental and more general reasons to determine which features of the nonequilibrium growth process are changed and unchanged by the anisotropy.

We find that immediately after the quench, the structure of the domains is very similar to that of the domains for zero field. However, the field breaks the symmetry in the different directions and, at later times, there is a crossover to strongly anisotropic domains. Satisfactory dynamical scaling is difficult to obtain, and we suggest reasons why this might be so. Nevertheless, we are able to conclude that the growth exponents in the two directions are different. More unexpectedly and more interestingly, the

inverse interfacial density, which is an *isotropic* measure of growth, seems to obey an extremely good power law and the growth exponent is 1/3 independent of the field strength. This isotropic length scale grows as a power law even in the temporal crossover regime from isotropic to very anisotropic domains. This result implies that a growth exponent of 1/3 may be a general consequence of the conservation law.

In the strong-field or long-time regime, the domains have a roughly triangular shape. The shapes of the domains can be understood in terms of a recently discovered surface driven interfacial instability.[14] The instability is not of the more familiar Mullin–Sekerka type, but is a localized instability due to fluxes along the interface. The surface driven instability depends on the orientation of the interface with respect to the field and helps explain why the final steady state consists of stripes parallel to the field. Triangular structures have also been observed in Monte Carlo simulations of driven diffusive systems.[13]

We also observe "bridge"-like structures connecting two domains of the same phase. The "bridge" acts like a solitary wave in that the structure moves with respect to the rest of the system at nearly constant velocity and maintains its size and shape for long periods of time. The "bridges" can be understood in terms of the dynamics of the one-dimensional driven diffusive system.

The remainder of the paper is organized as follows. In Section 2 we introduce the coarse-grained description of driven diffusive systems and the corresponding generalization of the Cahn–Hilliard equation. In Section 3 we report our numerical simulations of the phase separation dynamics. We describe the domain structure, the dynamical scaling behavior, and growth exponents in each direction. We study the dependence of dynamical scaling on the magnitude of the field and discuss the universality of the growth exponent for the isotropic length scale. In Section 4 we use an analysis of the stability of the interfaces to understand some of the structures found in the simulation. Section 5 is a summary.

2. THE CAHN–HILLIARD EQUATION FOR DRIVEN DIFFUSIVE SYSTEMS

The standard Cahn–Hilliard equation is a partial differential equation describing the dynamics of a system with a conserved order parameter.[18] In this section, we show how the equation must be modified in the presence of a field.

Assume a field of strength E in the x direction. Let $\psi(\mathbf{r}, t)$ be the local coarse-grained order parameter at point $\mathbf{r}$ and time t. For the lattice gas model ψ would be a coarse-grained local density. The evolution equation

for ψ is obtained by considering a closed system for which an equilibrium free energy exists. For periodic or open boundary conditions there is no such free energy. However, it is assumed that locally the dynamics is the same as that for the closed system. In the presence of a field the coarse-grained free energy is

$$F\{\psi\} = F_0\{\psi\} - E \int d\mathbf{r}\, x\psi(\mathbf{r}, t) \tag{2.1}$$

where F_0 is the coarse-grained free energy for zero field. However, the standard procedure for obtaining the Cahn–Hilliard equation for ψ results in E dropping out of the equation.[19] In other words, the field only affects the dynamics by modifying the boundary conditions. This is unphysical, as it implies that the effects of the field can be postponed for an arbitrary period of time by making the system arbitrarily large. However, in general the mobility depends on the local order parameter.[19] When this is included, the Cahn–Hilliard equation becomes

$$\frac{\partial \psi}{\partial t} = \nabla \cdot (M(\psi)\, \nabla \mu) - E \frac{\partial M(\psi)}{\partial \psi} \frac{\partial \psi}{\partial x} \tag{2.2}$$

where the zero-field chemical potential $\mu = \delta F_0\{\psi\}/\delta\psi$. We do not consider additional terms due to thermal fluctuations, since empirically it has been found that growth and scaling are not greatly affected by these thermal fluctuations.[20,22]

In general, F_0 is a complicated function of ψ. However, the scaling behavior does not depend on the exact form of F_0 as long as it has the correct overall features such as symmetry and types of extrema.[20,21] For Ising-like symmetry, we require a symmetric double-well potential. We choose the standard ψ^4 potential. The exact form of the mobility should also be unimportant. The simplest nontrivial form maintaining $\psi \to -\psi$ symmetry is $M = (1 - a\psi^2)/2$, where a is a parameter which depends on the temperature. Finally, we assume that the order-parameter-dependent mobility is only important in the coupling to the field.

With these assumptions, the evolution equation in the presence of a field is[7,8,19]

$$\frac{\partial \psi}{\partial t} = -\frac{1}{2}\nabla^2 \mu + E\psi \frac{\partial \psi}{\partial x} \tag{2.3}$$

where $\mu = \psi - \psi^3 + \nabla^2\psi$ and we have redefined $aE \to E$. Equation (2.3) is used as the starting point for our simulations and discussion of interfacial properties. This is the generalization of the Cahn–Hilliard equation for

driven diffusive systems. If E is interpreted as an electric field, the additional flux term is due to an order-parameter-dependent "conductivity."

There are several interesting features to note about Eq. (2.3). For $E=0$ we recover the standard Cahn–Hilliard equation. In one dimension and for $E \to \infty$, we obtain the Kuramoto–Sivashinsky equation, which is a deterministic model of phase turbulence.[23] Also, the field does not affect the linear behavior about the homogeneous $\psi=0$ state. Therefore, we expect that the behavior with finite E will be similar to the zero-field case for some time after the quench.

3. DYNAMICAL SCALING

3.1. Methods and Morphology

To study the dynamics of phase separation in the presence of a field, we have performed simulations of the Cahn–Hilliard equation for driven diffusive systems [Eq. (2.3)]. The system was prepared in the one-phase regime and immediately quenched into the two-phase coexistence regime. Domains of the two phases quickly formed, and we studied the growth of the domains with time.

The simulations were performed via an Euler discretization of Eq. (2.3) with time step $\delta t=0.25$ and a mesh size $\delta x=1.7$. The time step and mesh size were chosen as large as possible without affecting the quantities of interest. This was checked by limited simulations at smaller time steps and mesh sizes. (The simulations should be regarded as a lattice mapping and corresponds to the cell dynamical systems method of Oono and Puri.[21]

We used two-dimensional square lattices of size $N_x=1536$ in the x (field) direction and $N_y=128$ in the y direction. Periodic boundary conditions were used in each direction. The initial state was prepared by assigning to each site an uncorrelated random number chosen from a Gaussian distribution with variance of 0.02. The lattice mapping was updated to $t=7000$ (28,000 updates) for each initial condition, except for the zero-field case, where we only updated to $t=4000$. We averaged over 18 configurations for $E=0.4$, four configurations for $E=0.2$ and $E=0.1$, and one configuration for $E=0$.

Figure 1 shows a time sequence of the domain structure for $E=0.4$ for $t=62.5$ (250 updates), 500, 4000. At the earliest time ($t=62.5$) the observed patterns are isotropic ad very similar to the patterns found without a field.[15] This is because the linear instability about the small-amplitude initial state does not depend on E. At $t=500$ there is a clear anisotropy in the domain structure. We see the beginning of connected, roughly tri-

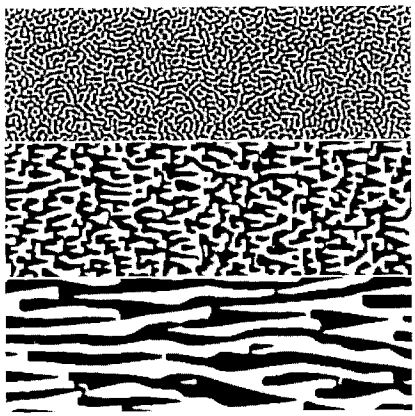

Fig. 1. The domain structure for $E=0.4$ at three different times $t=62.5$, $t=500$, and $t=4000$ (from top to bottom). The local order parameter is displayed on a gray scale with $\psi=+1$ black and $\psi=-1$ white. The field points to the right. A 384×128 portion of the full 1536×128 lattice is shown.

angularly shaped objects. The domains grow much faster in the direction of the field and become increasingly elongated with time ($t=4000$). We also see small "bridges" connecting two domains of the same phase. These bridges maintain their shape for long periods of time, moving at approximately constant velocity with respect to the rest of the pattern. Bridges connecting positive domains move in the direction of the field, while bridges connecting negative domains move in the opposite direction. For smaller values of the field, similar behavior is found. However, the patterns remain approximately isotropic for a longer period of time. This suggests that there is a crossover from isotropic to anisotropic patterns which might be described by a crossover time $\tau\sim E^{-\beta}$, $\beta>0$ being the crossover exponent.

Figure 2 shows the domain structures for an off-critical quench with average $\psi=-0.4$ and $E=0.4$. The triangular shape of the domains is more apparent since the domains are well separated from each other. The smaller domains move with respect to the larger ones. When a smaller domain approaches a larger one it is absorbed. This seems to be the dominant growth mechanism for off-critical quenches with $E\neq0$.

3.2. Isotropic Growth

To get an isotropic measure of the growth, we use the inverse interfacial area density. We identify a "broken bond" by a change in sign of the order parameter between nearest neighbor sites (in analogy with studies of

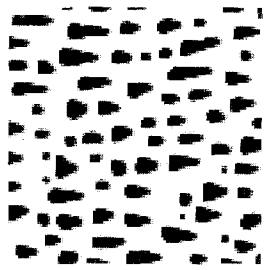

Fig. 2. The domain structure for an off-critical quench with average $\psi = -0.4$ and $t = 2000$. The roughly triangular shape of the domains is apparent.

the kinetic Ising model). Bonds can be oriented either parallel or perpendicular to the field. We define $B_x(t)$ as the number of "broken bonds" in the direction of the field. $B_y(t)$ is the corresponding number of broken bonds in the y direction. The isotropic length scale is

$$R_b(t) = \frac{2N_x N_y}{B_x(t) + B_y(t)} \tag{3.1}$$

For zero field, $R_b(t)$ is just a measure of the interfacial energy and grows as $t^{1/3}$. We choose this quantity since it has a simple physical meaning independent of whether dynamical scaling is observed or not.

Figure 3 shows $R_b(t)$ vs. t for four different values of the field. The lines are nonlinear least square fits to the data of the form $R(t) = R_0 + bt^{\alpha}$

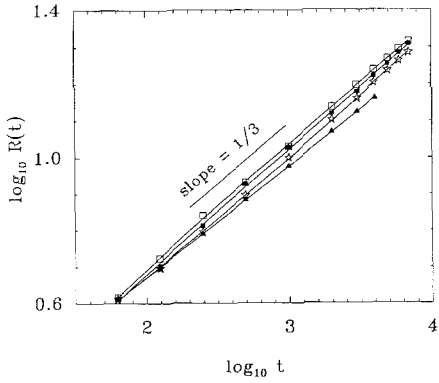

Fig. 3. The isotropic inverse interfacial density for $E = 0.4$ (open squares), $E = 0.2$ (filled squares), $E = 0.1$ (stars), $E = 0$ (triangles). The lines through the data points are fits to $R(t) = R(0) + bt^{\alpha}$. Here α ranges from 0.32 to 0.36 for different E. The statistical uncertainties are smaller than the symbol sizes.

and a line with slope 1/3 is drawn as a guide to the eye. We find an extremely good fit over more than two decades in time. R_0 depends on E and ranges from -0.6 to 0.4 (which is much less than the maximum R of about 25). At late times the lines are almost parallel, indicating that α for each one is very close to 1/3. The fitting procedure yields α between 0.32 and 0.36 for the various values of E. Therefore the data strongly suggest that the growth exponent for the isotropic length scale is 1/3 independent of the magnitude of E. Similarly, the off-critical quench yields structures that coarsen as $t^{1/3}$.

An asymptotic exponent of 1/3 may not be extremely surprising. What is unexpected is that the constant growth exponent of 1/3 shows no sign of the crossover from approximately isotropic to very anisotropic domains. This is surprising since power-law growth usually means that the dynamics is controlled by a single mechanism and that dynamical scaling is observed. However, the differences in the domain morphology seem to indicate that there is a crossover from one type of growth mechanism, controlled by surface tension at early times, to another, controlled by the field at late times. The fact that a power law growth is observed during this entire range of times indicates that there is an intricate coupling between the dynamics in the two directions.

Let us consider some arguments that might give a growth exponent of 1/3. One might hope to obtain the correct exponent by treating the growth in the x (field) and y directions separately. This line of argument suggests that, asymptotically, one of the two rates will dominate and determine the growth exponent for the isotropic length scale. However, it is difficult to see how such an argument can account for the 1/3 growth at early times and in the crossover regime.

The standard argument for a 1/3 exponent for conserved systems is based on the work of Lifshitz and Slyozov.[24] This argument, justified for off-critical quenches in the absence of a field, is based on competition between circular domains mediated by bulk diffusion and driven by surface tension. In our case the shape of domains is noncircular. Moreover, this shape changes with time. We suspect that the standard arguments for the 1/3 exponent may be overspecific. Our results indicate that there may be a more general argument using only the conservation law and some restrictions on the interactions (such as no hydrodynamic flow) which would be applicable whenever the domain sizes are much larger than the interfacial width. For example, it has already been shown that the 1/3 growth holds for spinodal decomposition, a situation far from that addressed by Lifshitz–Slyozov theory.[25,26] It is conceivable that a similar argument based on dimensional analysis of the relevant interface equations will provide an "explanation" of the growth law for $R_b(t)$.

3.3. Anisotropic Scaling

We discuss the anisotropic dynamical scaling using standard techniques. Our primary conclusion is that we do not observe satisfactory dynamical scaling in the separate directions during the regime that the homogeneous length scale $R_b(t)$ grows as $t^{1/3}$.

The anisotropy breaks the symmetry, so that the x and y directions may scale differently. As a result, scaling may be manifested in a variety of different ways. The most naive form of anisotropic scaling for the real-space correlation function is

$$C(x, y, t) = c(x/X(t), y/Y(t)) \tag{3.2}$$

where $X(t)$ and $Y(t)$ are measures of the characteristic length scales in the x and y directions. Dimensional arguments give the corresponding scaling form for the anisotropic scattering intensity,

$$S(k_x, k_y, t) = X(t)\, Y(t)\, G(k_x X(t), k_y Y(t)) \tag{3.3}$$

We measure three different sets of characteristic length scales: (1) the inverse of the first moments of the scattering intensity $K_x(t)^{-1}$ and $K_y(t)^{-1}$, where

$$K_x(t) = \frac{\int_0^\infty dk_x\, k_x S(k_x, 0, t)}{\int_0^\infty dk_x\, S(k_x, 0, t)} \tag{3.4}$$

and $K_y(t)$ is defined in a similar way. (2) The distances at which the correlation function drops to half its value at the origin, $X_c(t)$ and $Y_c(t)$, where

$$C(X_c, 0, t) = C(0, 0, t)/2 \tag{3.5}$$

and similarly for $Y_c(t)$. (3) The length scales associated with the interfacial area density, $X_b(t)$ and $Y_b(t)$, where

$$X_b(t) = N_x N_y / B_x(t) \tag{3.6}$$

and similarly for $Y_b(t)$. [Note that the isotropic length scale is given by $R_b(t)^{-1} = (X_b(t)^{-1} + Y_b(t)^{-1})/2$.]

Since the larger the field, the faster the crossover to the asymptotic behavior, we concentrate on the results for $E = 0.4$. Figure 4, which compares the time dependence of the x and y length scales, shows clear evidence of a crossover regime without any clean scaling behavior. This occurs despite the uniform power-law growth of the isotropic measure (shown in Fig. 3). In the direction of the field, x, the "effective" exponent

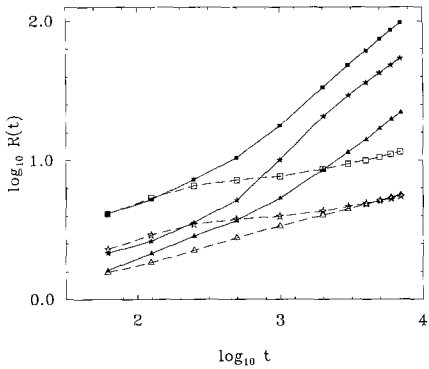

Fig. 4. Comparison of the length scales in the x (solid symbols with solid lines) and y direction (open symbols with dashed lines) for $E=0.4$. The symbols correspond to the bond (squares), correlation (stars), and scattering length scales (triangles).

increases from $\alpha \sim 1/3$ at early times to $\alpha \sim 0.8$–0.9 and the various length scales are not proportional. Similarly, the effective exponent for the y direction diminishes from $\alpha \sim 1/3$ to $\alpha \sim 1/4$. However, since $X_b(t)$ grows at a much faster rate than $Y_b(t)$, we expect that $Y_b(t) \sim R_b(t) \sim t^{1/3}$ as $t \to \infty$. This is a further indication that we are in a crossover regime.

Scaling is often analyzed using the real-space correlation function, which is shown in Fig. 5a (for the x direction). At earlier times $t < 125$

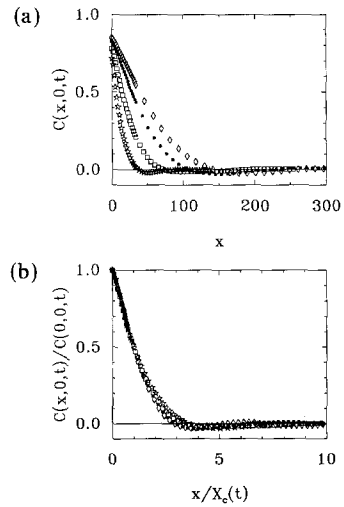

Fig. 5. (a) The correlation function $C(x, 0, t)$ along the x axis for $E=0.4$ and $t=1000$ (stars), 2000 (squares), 4000 (circles), and 6000 (diamonds). (b) The same data normalized by $C(0, 0, t)$ and plotted vs. $x/X_c(t)$.

one observes a correlation function much like that for zero field. With increasing t, the envelope of oscillations approaches the x axis, reflecting patterns with a broad distribution of domain lengths. Figure 5b shows the normalized, scaled correlation function. Although the data collapse for scaled distances $x/X_c(t) < 1/2$, dynamical scaling is violated at larger distances. Figure 6 shows the scaled form of the scattering intensity for the same times. The collapse of the data is poor for $t \leqslant 2000$. This is partially a reflection of an increasing asymmetry about the peak with time due to the anisotropy. The last two data sets show better collapse. This may be a sign that we are approaching a scaling regime, or it may simply be a consequence of the smaller ratio of times. The data do not show good enough collapse over a sufficient range of times for us to have any confidence that dynamical scaling is being observed.

Figure 7a shows the scaled scattering intensity in the k_y direction. In this direction the scattering intensity remains symmetric about the peak. Again the collapse of the data is poor. Figure 7b shows the corresponding scaled correlation function. The buildup of correlations in the y direction is implied by the decrease in oscillations in the x direction (Fig. 5). This is because local conservation of the order parameter requires that the integral of $C(x, y, t)$ over a region containing many domains must be nearly zero.

The conditions for dynamical scaling may be more difficult to obtain for the anisotropic case. Dynamical scaling is observed when the characteristic domain size is widely separated from any other length scale. For example, for the zero-field case, dynamical scaling will be observed when the average domain size $R(t)$ is much larger than the interfacial width. In the anisotropic case, such a separation of length scales may be elusive if the growth mechanisms in the x and y directions are coupled. This is because

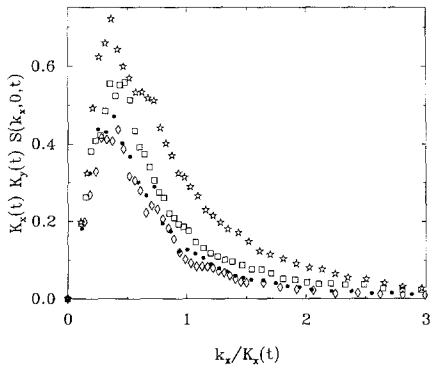

Fig. 6. The scaled scattering intensity along the k_x axis for $E = 0.4$ and the same times and symbols as in Fig. 5. Each point is an average over three k modes.

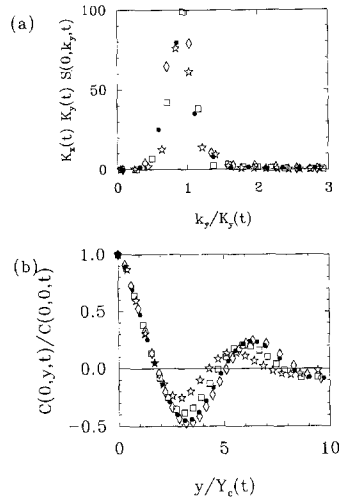

Fig. 7. (a) The scaled form of the scattering intensity along the k_y axis. (b) The normalized, scaled correlation function along the y direction. $E = 0.4$ and the times and symbols are the same as in Fig. 5.

some of the y length scale is projected into the x direction and vice versa. To illustrate how this may affect the scaling behavior, consider cigar-shaped domains with the long axis in the x direction. Assume that $X(t)$ grows faster than $Y(t)$ and that the tip of the cigar is a semicircle with radius $Y(t)$. In this case, rescaling the domain by $X(t)$ and $Y(t)$ will result in an increasingly rectangular object with time. Dynamical scaling will only occur when the curvature at the tip can be ignored relative to the rest of the domain, i.e., only when $X(t) \gg Y(t)$.

The crossover from isotropic to anisotropic domains depends on the magnitude of the field. Figure 8 compares the bond length scales for the different field strengths. The behavior of the y length scale is the most illuminating. Our results for the growth of the isotropic length scale tells us that the y length scale must grow as $t^{1/3}$ both at early times, before the anisotropy is important, and at later times, but with a smaller amplitude. The figure is consistent with our interpretation. As might be expected, the crossover occurs earlier for stronger fields. Even for the largest field, it is not clear if we have reached the asymptotic growth regime.

We can estimate the crossover time by balancing the portion of the Cahn–Hilliard equation without explicit field dependence ($M\nabla^2\mu$) with the additional flux term. In the absence of the field, $\nabla^2\mu \sim 1/R^3$, where R is the characteristic size of the domains. The flux term, on the other hand, scales

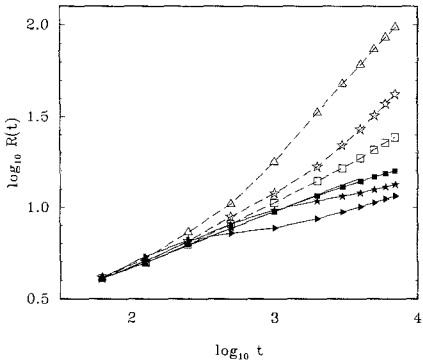

Fig. 8. The x (open) and y (filled) length scales for different electric fields. Open symbols are the x lengths $E=0.4$ (triangles), 0.2 (stars), 0.1 (squares). The heavy solid line is for $E=0$.

as E/R. The crossover should occur when $R \sim E^{-1/2}$. Since $R \sim t^{1/3}$, the crossover time τ behaves as $R^3 \sim E^{-\beta}$ with the exponent $\beta = 3/2$. Our data are consistent with this analysis, but are not sufficient for a complete test.

4. DOMAIN MORPHOLOGY

In this section we discuss the domain morphology obtained in the simulations. Figures 1 and 2 show a clear directional asymmetry in the domains as they become elongated. This asymmetry is a consequence of enhanced growth in the direction of the field. However, rather than forming ellipses, the domains assume a triangular shape. This is especially apparent in the off-critical quench (Fig. 2), where there is no percolation. (It should be noted that, in the absence of an external field, these domains would be nearly circular.[20]) The unusual triangular shape may be related to the intrinsic stability of interfaces with normal vectors oriented parallel and antiparallel to the field.[14] (Here we define the normal vector as pointing from the low-density phase, $\psi < 0$, to the high-density phase.)

In Fig. 9a we schematically show an isolated domain of high density in a background of low-density material. (This could represent, for example, one of the many domains in Fig. 2.) The local fluxes which result in mass transfer ultimately control the dynamics. In the absence of an external field, these local fluxes are a consequence of "local thermodynamic equilibrium" established at the interface (i.e., Gibbs–Thomson boundary conditions). Gradients in the chemical potential generate mass transfer through the bulk, causing the isolated domains to become circular (this process is discussed in detail in refs. 20 and 25). The presence of the field introduces a new mechanism of transport, which is related to the order-parameter-

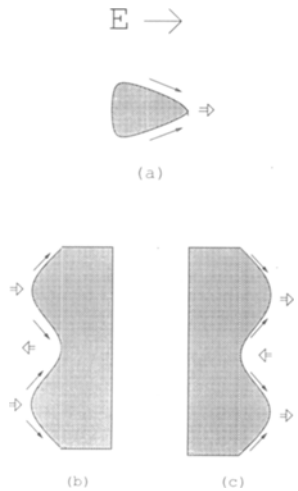

Fig. 9. (a) Schematic diagram showing the effect of the field on a triangular domain of phase $\psi > 0$ (cross-hatched). (b) A stable interface with respect to surface driven currents. (c) An unstable interface with respect to surface driven currents. The small arrows indicate the direction of ψ current along the interface. The large arrow indicate the motion of the domain. In each case the field acts to the right.

dependent mobility. Since this mobility $M \sim (1 - a\psi^2)$ is suppressed in the bulk, the increase in mass transfer will be concentrated along the interface. If this dominates the dynamics, there will be a tendency for matter to be transferred from the vertex of the triangle to the base (see Fig. 9a), causing the high-density domain to move with the field (for domains of low density, the process is reversed). In addition, the stability of the interface is affected by the field. As shown in Fig. 9b, if the normal to the interface is parallel to the field, the enhanced surface transport will stabilize the interface. On the other hand, if the normal is antiparallel (Fig. 9c), this mechanism will amplify small perturbations (analogous to a Raleigh instability). Thus, the vertex will become narrow because of the inherent instability of this orientation for the interface. However, the stable base will remain broad. (Note that the conventional Mullin–Sekerka instability, if present, would act to destabilize the base.[11])

For finite-size systems, the triangles will eventually elongate into stripes with interfaces whose normals are perpendicular to the field (assuming the system percolates). In fact, due to the surface driven instability, this is the only stable configuration for periodic boundary conditions. For other orientations, there will always be at least one unstable interface.

In order to verify these ideas, we have examined the evolution of an initially circular domain in the presence of a field. The domain elongates, assuming a roughly triangular shape, and the center of mass moves at a (nearly) constant velocity with the field. (In the absence of an external field, the circular domain would be stable and stationary.)

For the off-critical quench, the field-driven motion of the domains causes smaller ones (which move faster) to collide into the larger ones (which are nearly stationary). This seems to be the dominant growth mechanism. It should be noted that this contrasts sharply with previous off-critical simulations for $E=0$, where cluster motion is negligible, and growth proceeds by "evaporation and condensation" as described by Lifshitz and Slyozov.[24] It is very curious that both these simulations give a growth exponent of approximately 1/3.

The critical quench is much more difficult to understand because of the complicated percolation topology. Here the domains are no longer isolated and interdomain interactions play an important role. We have noticed that, when in close proximity, the vertex of one domain can influence the base of its neighbor. Figure 10a shows the resulting configuration. A bridge is formed which moves at nearly constant velocity while maintaining its shape for long periods of time. Figure 10b shows a cross

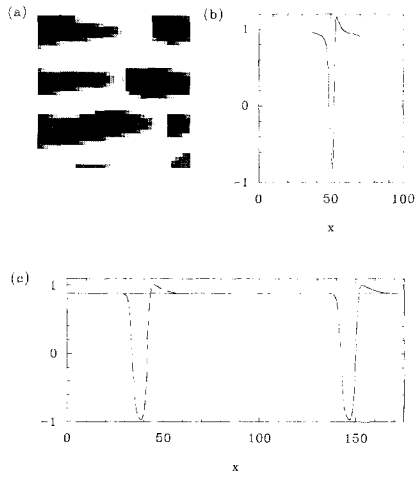

Fig. 10. (a) Enlarged view of the domain structure for $E=0.4$, showing the bridges separating the vertex of one (dark) domain from the base of its neighbor (there are three such bridges in this figure). (b) Profile of the order parameter across the central bridge. (c) Evolution of a one-dimensional solitary wave for $E=0.4$ and time difference $\delta t=2500$ (the dashed line represents the later time).

section of the bridge in the x direction. This bridge moves toward the vertex, causing that domain to shrink while the other grows correspondingly.

To understand these long-lived structures, we have considered the dynamics in one dimension. Beginning with the single-phase homogeneous state, we introduced small domains of the opposite phase. By numerically tracking the evolution, we observed the formation of "solitary waves" which move at a constant velocity and maintain their shape indefinitely as shown in Fig. 10c. The velocity depends on the width of the solitary wave, with wider ones moving more slowly. When the initial domain size approaches the interfacial width, the profile of these one-dimensional structures is similar to the profile of the two-dimensional bridge (see Fig. 10b). Therefore, we believe the two-dimensional bridges are a reflection of the one-dimensional dynamics.

5. SUMMARY

We have studied the behavior of a driven diffusive system (DDS) after a rapid quench. The field breaks the directional symmetry, causing a crossover from an initially isotropic to a strongly anisotropic morphology. Although the growths along and perpendicular to the field differ, we find that the inverse interfacial density, which is an *isotropic* measure, grows as $t^{1/3}$ independent of the field strength. This exponent is obtained throughout the crossover regime, even though dynamical scaling in the separate directions is not observed. Therefore, we expect that $t^{1/3}$ growth may be a more general consequence of the local conservation law than previously believed.

We have analyzed the dynamics in terms of a surface driven instability caused by the field. This instability generates roughly triangular domains. For off-critical quenches these domains coarsen through coalescence also with a growth exponent of 1/3. For critical quenches, domains, in part, interact through structures similar to one-dimensional solitary waves.

ACKNOWLEDGMENTS

We note that a similar system is being studied by S. Puri and K. Binder. We are very grateful to S. Puri for many useful discussions and for providing a preprint of their manuscript prior to publication. We would like to thank F. Briggs and J. D. Crawford for providing some of the computer time. D.J. and C.Y. are grateful to the National Science Foundation through the Division of Materials Research under Grant No. DMR89-14621. T.R. would like to thank NSERC of Canada for financial support. A.H.M. and D.J. also thank NATO for partial support under the

Collaborative Research Grant No. 900328. A.H.M. also acknowledges the support of the Direccion General de Investigacion Cientifica y Tecnica (Spain) Pro. No. PBR87-0014.

REFERENCES

1. H. Spohn, *Ann. N. Y. Acad. Sci.* **491**:157 (1987); J. Marro, in *Fluctuations and Stochastic Phenomena in Condensed Matter*, L. Garrido, ed. (Springer-Verlag, 1987); B. Schmittmann, *Int. J. Mod. Phys. B* **4**:2269 (1990).
2. J. B. Bates and G. C. Farrington, eds., *Fast Ionic Transport in Solids* (North-Holland, New York); *Solid State Ionics* **5** (1981); W. Dieterich, P. Fulde, and I. Peschel, *Adv. Phys.* **29**:527 (1980).
3. S. Katz, J. L. Lebowitz, and H. Spohn, *Phys. Rev. B* **28**:1655 (1983); *J. Stat. Phys.* **34**:497 (1984); J. Marro, J. L. Lebowitz, H. Spohn, and M. H. Kalos, *J. Stat. Phys.* **38**:725 (1985).
4. L. Vallés and Marro, *J. Stat. Phys.* **43**:441 (1986); L. Vallés and Marro, *J. Stat. Phys.* **49**:89 (1987); J. Marro and J. L. Vallés, *J. Stat. Phys.* **49**:121 (1987); J. Marro, J. L. Vallés, and J. M. Gonzalez-Miranda, *Phys. Rev. B* **35**:3372 (1987).
5. H. van Beijeren and L. S. Schulman, *Phys. Rev. Lett.* **53**:806 (1984).
6. J. Krug, J. L. Lebowitz, H. Spohn, and M. Q. Zhang, *J. Stat. Phys.* **44**:535 (1986); M. Q. Zhang, *Phys. Rev. A* **35**:2266 (1987); R. Dickman, *Phys. Rev. A* **38**:2588 (1988).
7. H. K. Janssen and B. Schmittmann, *Z. Phys. B* **63**:517; **64**:503 (1986).
8. H. van Beijeren, R. Kutner, and H. Spohn, *Phys. Rev. Lett.* **54**:2026 (1985); K.-T. Leung and J. L. Cardy, *J. Stat. Phys.* **44**:567 (1986).
9. K.-T. Leung, *J. Stat. Phys.* **50**:405 (1988).
10. A. Hernandez-Machado and D. Jasnow, *Phys. Rev. A* **37**:656 (1988); A. Hernandez-Machado, H. Guo, J. L. Mozos, and D. Jasnow, *Phys. Rev. A* **39**:4783 (1989).
11. K.-T. Leung, *J. Stat. Phys.* **61**:345 (1990).
12. K.-T. Leung, K. K. Mon, J. L. Vallés, and R. K. P. Zia, *Phys. Rev. Lett.* **61**:1744 (1988); J. L. Vallés, K.-T. Leung, and R. K. P. Zia, *J. Stat. Phys.* **56**:43 (1989).
13. D. H. Boal, R. P. K. Zia, and B. Schmittmann, *Phys. Rev. A* **43**:5214 (1991).
14. T. Rogers, A. Hernandez-Machado, and D. Jasnow, in preparation.
15. J. D. Gunton, M. San Miguel, and P. S. Sahni, in *Phase Transitions and Critical Phenomena*, Vol. 8, C. Domb and J. L. Lebowitz, eds. (Academic Press, New York, 1983), p. 267; H. Furukawa, *Adv. Phys.* **34**:703 (1985); K. Binder, in *Phase Transformations of Materials (Materials Science and Technology)*, Vol. 5, P. Haasen, ed. (Springer-Verlag, Berlin, 1991), p. 405.
16. M. R. Moldover, J. V. Sengers, R. W. Gammon, and R. J. Hocken, *Rev. Mod. Phys.* **51**:79 (1979).
17. M. Q. Zhang, J.-S. Wang, J. L. Lebowitz, and J. L. Vallés, *J. Stat. Phys.* **52**:1461 (1988); P. L. Garrido, J. L. Lebowitz, C. Maes, and H. Spohn, *Phys. Rev. A* **42**:1954 (1990); G. Grinstein, D. H. Lee, and S. Sachdev, *Phys. Rev. Lett.* **64**:1927 (1990).
18. J. W. Cahn and H. E. Hilliard, *J. Chem. Phys.* **28**:258 (1958); H. E. Cook, *Acta Metall.* **18**:297 (1970).
19. K. Kitahara, Y. Oono, and D. Jasnow, *Mod. Phys. Lett. B* **2**:765 (1988).
20. T. R. Rogers and R. C. Desai, *Phys. Rev. B* **39**:11956 (1989); K. E. Elder, T. M. Rogers, and R. C. Desai, *Phys. Rev. B* **38**:4725 (1988).
21. Y. Oono and S. Puri, *Phys. Rev. Lett.* **58**:836 (1988); S. Puri and Y. Oono, *Phys. Rev. A* **38**:1542 (1988).

22. Y. Oono and S. Puri, *Mod. Phys. Lett. B* **2**:861 (1988); C. Roland and M. Grant, *Phys. Rev. Lett.* **60**:2657 (1988); A. J. Bray, *Phys. Rev. Lett.* **62**:2841 (1989).
23. K. Kuramoto and T. Tsuzuki, *Prog. Theor. Phys.* **55**:356 (1976); G. Sivashinsky, *Acta Astronautica* **4**:1117 (1977).
24. I. M. Lifshitz and V. V. Slyozov, *J. Phys. Chem. Solids* **19**:35 (1961).
25. K. Kawasaki and T. Ohta, *Physica A* **118**:175 (1983); K. Kawasaki, *Ann. Phys.* **154**:319 (1984).
26. E. D. Siggia, *Phys. Rev. A* **20**:595 (1979).